



Cite this: DOI: 10.1039/d5fb00413f

## Enhancing millet-based analogue rice through sustainable cold plasma treatment: effects on mineral composition, structural, textural, cooking, and rheological properties

S. Ganga Kishore,<sup>a</sup> Madhuresh Dwivedi, <sup>\*a</sup>R. Rahul, <sup>b</sup>J. Deepa,<sup>c</sup> G. Jeevarathinam, <sup>\*d</sup>K. Kamaleeswari,<sup>a</sup> Gitanjali Jothiprakash<sup>e</sup> and Abinaya Veluswamy<sup>e</sup>

This study investigates the effects of cold plasma treatment on extruded millet-based analogue rice (MAR), formulated using pearl millet, sorghum, and parboiled rice. The treatment was applied at varying voltages (10, 20, and 30 kV) and time durations (10, 20, and 30 minutes) to evaluate its impact on physicochemical, cooking, and functional properties. The parameters assessed include color difference ( $\Delta E$ ), water absorption index (WAI), cooking loss (CL), water absorption ratio (WAR), cooking time (CT), and water solubility index (WSI). The results indicated that the highest treatment voltage (30 kV) and time duration (30 minutes) resulted in a minimized  $\Delta E$  of  $2.16 \pm 0.30$ , reduced CT of  $22.16 \pm 0.37$  minutes, decreased CL of  $6.62 \pm 0.28\%$ , maximum WAI of  $4.52 \pm 0.27 \text{ g g}^{-1}$ , maximum WAR of  $4.31 \pm 0.26$ , and a minimum WSI of  $2.16 \pm 0.30 \text{ g g}^{-1}$ . Cold plasma treatment induced significant molecular modifications in MAR, evident from shifts in FTIR peaks and intensities, indicating structural alterations in starch molecules. Additionally, notable improvements in mineral composition, pasting behavior, and textural characteristics were observed, demonstrating statistical significance ( $p < 0.05$ ). XRD analysis revealed reduced relative crystallinity in treated MAR, signifying improved structural stability. Microstructural analysis showed untreated MAR with a smooth surface and minimal porosity, while treated samples exhibited rougher, more porous surfaces due to moisture removal and starch rearrangement. These findings demonstrate that cold plasma offers a sustainable, non-thermal, and chemical-free processing alternative that improves the quality and functionality of millet-based analogue rice, aligning with current efforts toward environmentally friendly, energy-efficient, and nutritionally enhanced food technologies.

Received 22nd July 2025  
Accepted 24th November 2025

DOI: 10.1039/d5fb00413f  
[rsc.li/susfoodtech](http://rsc.li/susfoodtech)



### Sustainability spotlight

This study highlights the transformative potential of cold plasma (CP) technology as a sustainable and non-thermal processing method to enhance the quality of millet-based analogue rice (MAR) formulated from pearl millet, sorghum, and parboiled rice. CP treatment at varying voltages and time combinations significantly improved cooking quality, hydration capacity, textural properties, and rheological behavior. Notable enhancements included reduced cooking loss and time, increased water absorption, and greater structural stability, supported by reduced crystallinity and starch molecular reorganization. Analytical techniques such as FTIR, XRD, and SEM confirmed substantial starch modification and microstructural alterations, contributing to improved functional and physical attributes. These findings underscore the potential of cold plasma as a green and energy-efficient technology for developing nutrient-dense and structurally stable millet-based rice analogues aligned with the goals of future-ready functional food systems.

## 1. Introduction

Millets are highly valued nutri-cereals, abundant in minerals, vitamins, bioactive compounds, and dietary fiber, and are recognized for their anti-cancer, anti-inflammatory, and anti-oxidant properties which can reduce the risk of cancer, type 2 diabetes, celiac disease, obesity, gastrointestinal problems, and cardiovascular diseases.<sup>1,2</sup> These gluten-free grains with a low glycaemic index are an excellent source of essential nutrients containing iron, zinc, copper, potassium, phosphorus, and

<sup>a</sup>Department of Food Process Engineering, National Institute of Technology, Rourkela, Odisha, 769 008, India. E-mail: madhureshd@gmail.com

<sup>b</sup>Department of Food Technology, Dhanalakshmi Srinivasan College of Engineering, Coimbatore-641 105, Tamil Nadu, India

<sup>c</sup>Department of Food Technology, Nehru Institute of Technology, Coimbatore-641 105, Tamil Nadu, India

<sup>d</sup>Department of Food Technology, Hindusthan College of Engineering and Technology, Coimbatore-641 032, Tamil Nadu, India. E-mail: jeevaganesan.tnau@gmail.com

<sup>e</sup>Centre for Post-Harvest Technology, Tamil Nadu Agricultural University, Coimbatore-641 003, Tamil Nadu, India

calcium, offering a sustainable approach for addressing malnutrition and metabolic disorders worldwide.<sup>3</sup> Millets hold significant potential for developing nutraceutical-based and functional food products with extensive health benefits and can be used in making a variety of dishes, including noodles, soups, drinks, pancakes, porridges, etc.<sup>4</sup>

The global millet production reached 32.09 million metric tons during the year 2022–2023, in which India was the leading producer, contributing 13.51 million metric tons, followed by Niger and China.<sup>3</sup> However, millets are still regarded as “underutilized” or “neglected” crops due to the increase in consumption of other cereals like wheat and rice, which align with changing taste preferences and the demand for quicker preparation times, particularly in urban areas.<sup>5</sup> Other limitations of millets include inferior cooking quality, coarse texture, lack of processing machinery, insufficient research, minimal use in convenience foods, and a lack of innovative approaches to food product development.<sup>6,7</sup>

The inferior cooking quality of millets is due to the presence of native starch, a natural polymer with semicrystalline granules, composed of amylose (a linear biopolymer of  $\alpha$ -D-glucose linked by  $\alpha$ -1,4-glycosidic bonds) and amylopectin (a branched biopolymer with  $\alpha$ -1,4- and  $\alpha$ -1,6-glycosidic bonds), which has poor water solubility, limited shear, and thermal stability, leading to significant limitations on its physical characteristics and functional properties.<sup>8</sup> These limitations can be addressed by modifying starch to enhance its cooking, physicochemical, functional, thermal, and structural properties.<sup>9</sup> Starch modification can be achieved through various methods, including physical,<sup>10</sup> chemical,<sup>11</sup> and biological<sup>12</sup> approaches, as well as through combinations<sup>13</sup> of these techniques. Among these techniques, physical modification has gained notable attention recently as it is pollution free, safe, simple, and clean.<sup>14</sup>

Cold plasma (CP) is an emerging, innovative, nonthermal, and sustainable technology that has gained attention in recent years as a physical method to modify starch due to its environmental friendliness, solvent-free nature, minimal by-product generation, ease of use, and higher efficiency.<sup>15</sup> The starch modification using cold plasma primarily involves the generation of free radicals and energy-driven electron-induced chemical reactions which results in depolymerization of starch chains, plasma etching, cross-linking, and the creation of new functional groups.<sup>16</sup> Current studies have shown that cold plasma can effectively alter the functional<sup>17</sup> and physicochemical<sup>10</sup> properties of starch, thereby improving the hydrophobic properties, water binding capacity, pasting behaviour, swelling power, and solubility.<sup>18,19</sup> It also reduces the peak viscosity and lowers the gelation temperature of starch.<sup>20,21</sup> Studies have reported that lower intensity plasma treatment of pearl millet and sorghum results in cross-linking, while depolymerisation occurs at a higher intensity of plasma treatment.<sup>22,23</sup>

Recent studies related to the effect of cold plasma treatment on rice grains,<sup>24</sup> brown rice,<sup>25,26</sup> lightly-milled rice<sup>27,28</sup> and contaminated rice.<sup>29</sup> However, no published literature currently exists on the application of CP to millet-based analogue rice (MAR). In this regard, the current study aimed to evaluate the effect of cold plasma treatment on millet-based analogue rice

(MAR) developed using pearl millet, sorghum, and parboiled rice to understand the significant changes occurring in its cooking characteristics, physicochemical properties, textural properties, pasting behaviour, and rheological properties. The study also sought to analyse changes in morphology, functional groups, and relative crystallinity to assess the impact of cold plasma on starch modification. The novelty of this study lies in the first-time application of cold plasma technology to enhance millet-based analogue rice, providing a sustainable and energy-efficient processing strategy that supports circular bioeconomy principles and fosters the development of resilient, health-focused, and environmentally responsible food systems.

## 2. Materials and methods

### 2.1. Raw material procurement

The raw materials such as pearl millet, sorghum, and parboiled rice were purchased from Suruchi market, Rourkela, Odisha, India. These grains were cleaned and milled using a hammer mill (model: Indosaw Products Pvt. Ltd, Haryana, India) to produce respective flours, which were then sifted through a sieve shaker (Shiva Scientific Instruments, Delhi) to achieve a particle size of less than 300  $\mu\text{m}$ . The respective flours were then stored in air-tight polyethylene bags to ensure their preservation.

### 2.2. Formulation of millet-based analogue rice

Millet-based analogue rice was produced using a 1 kg blend of multigrain flour, consisting of 610 g pearl millet flour, 270 g sorghum flour, and 120 g parboiled rice flour. The respective flours were then blended using a planetary mixer (Jinan Saibainuo Machinery Co., Ltd) for 30 minutes at a speed of 400 rpm. The mixture was then adjusted to a moisture content of 28% w.b. and stored overnight at 4 °C to allow the moisture to equilibrate. The prepared blend was further processed using a pilot-scale twin-screw extruder (SYSLG32, Jinan Saibainuo, China) with the processing conditions of 720 rpm screw speed, 420 rpm feeder speed, 2700 rpm cutter speed, and 80 °C die temperature. The produced millet-based analogue rice was then dried using a recirculating dryer (Servo Enterprises, Chennai) at 60 °C until it reached a final moisture content of 12% w.b.

### 2.3. Experimental design for cold plasma treatment

The experimental plan was designed using different combinations of the independent variables which include treatment voltage (10, 20 and 30 kV) and treatment time (10, 20 and 30 minutes). The dependent variables include total colour change ( $\Delta E$ ), water absorption index (WAI), water solubility index (WSI), cooking time (CT), water absorption ratio (WAR), and cooking loss (CL). The final formulation for the cold plasma treatment was determined using the best results obtained from the dependent variables of different composition trials. The experiment was performed using a multipin discharge plasma reactor (IN-HVLT MP, Ingenium Naturae Private Limited, Gujarat, India), operating with an input voltage of 230 V at 50 Hz and a high output voltage of 60 kV. It had a discharge area of 185



× 250 mm and featured a high-voltage electrode with 63 stainless steel pins arranged in a 9 × 7 matrix. The stainless-steel electrodes ensure durability and longevity. All experiments were conducted at atmospheric pressure using ambient air as the working gas. While the composition of ambient air (approximately 78% nitrogen, 21% oxygen, and 1% other gases) can vary and influence the generation of plasma-induced reactive oxygen and nitrogen species (RONS), the relative humidity was continuously monitored throughout the experiments and recorded as 65.3% ± 1.2% to ensure consistent treatment conditions and improve reproducibility. A consistent inter-electrode distance of 3 cm was maintained throughout all trials.

#### 2.4. Colour measurement

The colour value of the samples was measured using a Hunter Lab colorimeter (ColorFlex EZ, Hunter Lab, Virginia, USA), which was calibrated with black and white reference standards. The readings were taken in triplicate, evaluating the color parameters in terms of  $L^*$  (blackness to whiteness),  $a^*$  (redness to greenness), and  $b^*$  (blueness to yellowness) values. The changes in the colour intensity ( $\Delta E$ ) were calculated using eqn (1) as reported by Bohlooli *et al.*<sup>29</sup>

$$\Delta E = \sqrt{(\Delta L)^2 + (\Delta a)^2 + (\Delta b)^2} \quad (1)$$

#### 2.5. Water absorption and the solubility index

A sample of 1 g was mixed with 12 mL of deionized water in a centrifugal tube. The mixture was then incubated at 30 °C in a shaking water bath for 30 minutes. After incubation, the mixture was further centrifuged at 3000g for 10 minutes. The supernatant was carefully transferred into a pre-weighed weighing bottle and then dried at 105 °C until a constant weight was achieved. The water absorption index (WAI) and water solubility index (WSI) were determined using eqn (2) and eqn (3) as described by Zeng *et al.*<sup>26</sup>

$$\text{WAI (g g}^{-1}\text{)} = \frac{W_{\text{RP}}}{W_{\text{IDS}}} \quad (2)$$

$$\text{WSI (\%)} = \frac{W_{\text{DS}}}{W_{\text{IDS}}} \times 100 \quad (3)$$

where  $W_{\text{RP}}$ ,  $W_{\text{DS}}$  and  $W_{\text{IDS}}$  represent the weight of residual precipitate, dry solids in the supernatant and initial dried sample in g.

#### 2.6. Cooking time

A sample of 5 g was added into a test tube with 20 mL of distilled water and subjected to a boiling water bath for cooking. The initial time was recorded, and every 30 seconds, a small portion of the sample was removed and pressed between two glass slides to determine the disappearance of the white core. The cooking time was noted when the sample was fully cooked and no longer displayed a white core.<sup>27</sup>

#### 2.7. Cooking loss and the water absorption index

A sample of 5 g was cooked in 20 mL of boiling distilled water in a water bath. After cooking, the leached solids were separated and transferred to a glass Petri dish, and dried at 105 °C in a hot air oven for 24 h. The weights of both the sample and the dried leached solids were measured using a weighing balance. The water absorption ratio and cooking loss were determined following the procedure reported by Nithya *et al.*<sup>30</sup>

#### 2.8. Textural analysis

A typical two compression cycle procedure was carried out for the cooked rice samples using a 38.1 mm cylindrical probe applying a compressive strain of 75% relative to the initial height of the rice kernel layer (1.7 ± 0.3 mm). Ten rice kernels were arranged in a single layer on the instrument base. A texture analyser (CT3, Brookfield Engineering, USA) was used to assess the textural properties such as cohesiveness, hardness, adhesiveness, gumminess, springiness, and chewiness as stated by Yadav *et al.*<sup>31</sup>

#### 2.9. Rheological properties

The rice samples, weighing 5 g each, were mixed with 15 mL of deionized water and then heated in a water bath for 20 minutes at 95 °C for complete gelatinization. Following the gelatinisation process, the cooked samples were compressed in the angular frequency range of 0.01 Hz to 100 Hz using a mold that was placed in a rheometer (MCR 102e, Anton Paar Instruments, Austria) with a 1 mm spacing. Rheological characteristics in terms of shear stress, shear rate, viscosity, storage modulus ( $G'$ ) and loss modulus ( $G''$ ) were measured as given by Wang *et al.*<sup>32</sup>

#### 2.10. Pasting properties

A sample of 2 g was mixed with 25 mL of distilled water using plastic paddles in metal canisters and then analyzed using compact rheometer (model: MCR 302e, Anton Paar, Austria). The sample was initially maintained at 50 °C for 1 minute. It was subsequently heated to 95 °C and held at this temperature for 3 minutes. After this period, the heated sample was cooled down to 50 °C and then maintained at 50 °C for an additional 2 minutes. The pasting properties in terms of peak viscosity, breakdown viscosity, setback from trough, setback from peak, final viscosity, peak temperature, pasting temperature, peak time and holding strength were determined as reported by Wang *et al.*<sup>33</sup>

#### 2.11. FTIR analysis

The rice samples were analysed using an FTIR spectrometer (Alpha E, Vertex 70, Bruker Optics, Inc., Billerica, MA, Germany). The spectra measurement was done at 25 °C between 400 and 4000  $\text{cm}^{-1}$  using the pellets made by hydraulically pressing a combination of 5 mg of the rice sample and 100 mg of potassium bromide as reported by Nithya *et al.*<sup>30</sup>



## 2.12. X-ray diffraction analysis

The rice samples were subjected to X-ray diffraction pattern analysis using an X-ray diffractometer (Philips PAN analytical, USA). During the analysis, a diffraction angle of 5–40° and a scan rate of 2.68° min<sup>-1</sup> were used. The percentage of relative crystallinity was determined using eqn (4) as reported by Nithya *et al.*<sup>30</sup>

$$\text{Relative crystallinity (\%)} = \frac{C_{\text{Peak area}}}{C_{\text{Peak area}} + A_{\text{area}}} \times 100 \quad (4)$$

where  $A_{\text{area}}$  denotes the amorphous area and  $C_{\text{Peak area}}$  denotes the crystalline peak area.

## 2.13. Scanning electron microscopy analysis

The surface microstructure of the rice samples was examined using a scanning electron microscope (JSM-6480LV, SEM, JEOL, Germany). The samples were placed on the pin stubs, covered with a layer of gold palladium, and adhered with carbon tape. The images were taken at magnification levels of 70 $\times$  and 2000 $\times$  as reported by Vishwakarma *et al.*<sup>34</sup>

## 2.14. Elemental analysis of MAR

The elements present in the samples were analysed using an inductively coupled plasma mass spectrometer (model – Thermo Scientific™ ICAP™ RQ, type – single quadrupole ICP-MS, hertz – 2 MHz, nebulizer – borosilicate glass, spray chamber – quartz, cyclonic). The elemental composition of <sup>23</sup>Na (sodium), <sup>24</sup>Mg (magnesium), <sup>31</sup>P (phosphorus), <sup>39</sup>K (potassium), <sup>44</sup>Ca (calcium), <sup>48</sup>Ti (titanium), <sup>52</sup>Cr (chromium), <sup>55</sup>Mn (manganese), <sup>57</sup>Fe (iron), <sup>60</sup>Ni (nickel), <sup>63</sup>Cu (copper), <sup>66</sup>Zn (zinc), and <sup>95</sup>Mo (molybdenum) in MAR samples was evaluated using a standard ICP-MS procedure as reported by Novotnik *et al.*<sup>35</sup>

## 2.15. Statistical analysis

The data were analysed using SPSS statistical software (ver. 27.0; SPSS Inc., Chicago, IL, USA). One-way analysis of variance (ANOVA) was performed to determine the statistical

significance. The mean values and standard error of the mean are reported. The significance of the data was detected and the difference among the mean values was determined by performing the *T*-test at a confidence level of  $p < 0.05$ .

## 3. Results and discussion

### 3.1. Effect of cold plasma treatment on cooking and functional properties of MAR

Different combinations of cold plasma treatment (CPT) voltage and exposure time were applied to MAR to evaluate their effects on functional and physicochemical properties such as water absorption index (WAI), total colour change ( $\Delta E$ ), water solubility index (WSI), cooking loss (CL), water absorption ratio (WAR), and cooking time (CT). These properties serve as important indicators of structural and molecular transformations induced by non-thermal plasma exposure.<sup>20</sup> The obtained effects of CPT for the different combinations of treatment are given in Table 1. Significant variations in colour change ( $\Delta E$ ) were observed among the treatments. The highest  $\Delta E$  ( $20.47 \pm 0.41$ ) occurred at 20 kV for 30 minutes, while the lowest value ( $2.16 \pm 0.19$ ) was found at 30 kV for 30 minutes. This suggests that at moderate voltages the plasma promotes surface oxidation and partial degradation of pigments or phenolic compounds, leading to visible discolouration. However, higher voltages may induce cross-linking of surface macromolecules or polymer rearrangement that suppresses light scattering and leads to a less noticeable colour change.<sup>36,37</sup> This phenomenon is attributed to the presence of reactive oxygen and nitrogen species (RONS) (such as ozone ( $O_3$ ), hydroxyl radicals ( $-OH$ ), and nitric oxide ( $NO^+$ )) generated during plasma discharge which can interact with chromophores or proteins and alter surface reflectivity.<sup>38</sup>

WAI values varied between  $3.61 \pm 0.29$  and  $5.10 \pm 0.18$  g g<sup>-1</sup> dry solid. The highest WAI was recorded in the sample treated at 10 kV for 30 minutes suggesting that mild plasma treatment may enhance porosity and surface roughness, improving water uptake. Conversely, at higher voltages and longer durations, a reduced WAI could result from structural compaction or

Table 1 Effect of cold plasma treatment on cooking and functional properties of millet-based analogue rice (MAR)<sup>a</sup>

Sr. no.	Sample	$\Delta E$	WAI (g water per g dry solid)	WSI (g water per 100 g dry solid)	CT (minutes)	WAR	CL (%)
1	10 kV, 10 min	$19.15 \pm 0.49^f$	$3.61 \pm 0.30^a$	$19.15 \pm 0.20^f$	$25.43 \pm 0.49^h$	$4.92 \pm 0.24^d$	$10.15 \pm 0.20^e$
2	10 kV, 20 min	$4.34 \pm 0.36^d$	$4.67 \pm 0.31^b$	$4.34 \pm 0.39^d$	$24.1 \pm 0.46^g$	$4.88 \pm 0.30^{cd}$	$8.2 \pm 0.51^c$
3	10 kV, 30 min	$2.39 \pm 0.27^{ab}$	$5.1 \pm 0.30^c$	$2.39 \pm 0.31^{ab}$	$21.84 \pm 0.37^{bc}$	$4.8 \pm 0.27^{cd}$	$10.56 \pm 0.35^f$
4	20 kV, 10 min	$2.48 \pm 0.44^{ab}$	$4.64 \pm 0.32^b$	$2.48 \pm 0.48^{ab}$	$23.45 \pm 0.29^e$	$4.51 \pm 0.45^{bc}$	$11.19 \pm 0.39^g$
5	20 kV, 20 min	$10.43 \pm 0.39^e$	$4.52 \pm 0.24^b$	$10.43 \pm 0.35^e$	$21.48 \pm 0.54^b$	$3.5 \pm 0.24^a$	$9.54 \pm 0.27^d$
6	20 kV, 30 min	$20.47 \pm 0.39^g$	$4.43 \pm 0.45^b$	$20.47 \pm 0.28^g$	$22.43 \pm 0.46^d$	$4.66 \pm 0.31^{bcd}$	$8.37 \pm 0.30^c$
7	30 kV, 10 min	$3.22 \pm 0.33^c$	$4.69 \pm 0.30^b$	$3.22 \pm 0.36^c$	$23.45 \pm 0.44^f$	$4.83 \pm 0.28^{cd}$	$6.47 \pm 0.27^a$
8	30 kV, 20 min	$2.65 \pm 0.32^b$	$4.62 \pm 0.46^b$	$2.65 \pm 0.27^b$	$20.36 \pm 0.28^a$	$4.61 \pm 0.21^{bcd}$	$7.46 \pm 0.34^b$
9	30 kV, 30 min	$2.16 \pm 0.30^a$	$4.52 \pm 0.27^b$	$2.16 \pm 0.30^a$	$22.16 \pm 0.37^{cd}$	$4.31 \pm 0.26^b$	$6.62 \pm 0.28^a$
F-Value		2357.473**	7.696**	2879.716**	76.737**	13.292**	154.151**

<sup>a</sup> Results are expressed as mean  $\pm$  SD ( $n = 3$ ). Values in the same row with different letters (a–g) are significantly different at  $p < 0.05$  (\*\* denotes high significance).



surface hardening caused by plasma-induced cross-linking of starch and protein molecules.<sup>39</sup> These structural alterations are consistent with plasma-induced partial denaturation or oxidation of surface molecules that reduce their water-binding capacity.<sup>40</sup> The water solubility index (WSI) ranged from  $2.16 \pm 0.19$  to  $20.47 \pm 0.41$  g per 100 g dry solid. The highest WSI was found in samples treated at 20 kV for 30 minutes, likely due to partial depolymerization of starch and protein components. Plasma-generated radicals can cleave glycosidic and peptide bonds leading to smaller water-soluble fragments.<sup>41,42</sup> However, at 30 kV for 30 minutes the WSI decreased significantly suggesting that excessive energy input may promote aggregation or re-polymerization of degraded components by reducing solubility.<sup>22</sup>

Cooking time (CT) showed a downward trend with increasing plasma intensity ranging from  $25.43 \pm 0.07$  minutes at 10 kV for 10 minutes to  $20.36 \pm 0.07$  minutes at 30 kV for 20 minutes. The shortened CT observed at higher voltages may be due to disruption of starch crystallinity and weakening of intermolecular hydrogen bonding, which facilitate quicker gelatinization during thermal processing.<sup>43,44</sup> Plasma treatment likely disrupts double helices in amylopectin and partially opens up granules increasing water and heat penetration. Water absorption ratio (WAR) values ranged from  $3.50 \pm 0.025$  to  $4.92 \pm 0.06$ . The highest WAR was observed in samples treated at 10 kV for 10 minutes reflecting enhanced water absorption due to minimal structural damage and preservation of hydrophilic functional groups. The WAR declined as voltage and exposure time increased, likely due to plasma-induced hydrophobic layer formation or densification of the grain matrix that restricted water uptake.<sup>45</sup> Such modifications may stem from surface oxidation of polysaccharides and proteins leading to decreased porosity and reduced swelling capacity. These results show that CPT significantly alters the physical characteristics of MAR *via* mechanisms involving oxidation, fragmentation, cross-linking, and thermal mimicry. Moderate treatment (*e.g.*, 20 kV, 30 minutes) favours depolymerization and increased solubility, while higher intensity treatment (*e.g.*, 30 kV, 30 minutes) favours surface restructuring and cross-linking, resulting in reduced solubility and colour change. The interdependence of the WAI and WSI indicates that plasma-mediated molecular changes govern water interactions particularly through the breakdown or modification of biopolymeric structures like starch and protein.<sup>46</sup>

Cooking loss (CL), which reflects the percentage of material lost during thermal processing, varied notably across treatments ranging from 6.47% to 11.19%. It indicates a clear influence of the voltage intensity and duration. The highest CL was observed in the sample treated at 20 kV for 10 minutes (11.19%), suggesting excessive structural disruption under these conditions. It is likely due to over-electroporation leading to weakened protein matrices and increased leaching of water and soluble solids.<sup>47</sup> In contrast, the lowest CL was recorded at 30 kV for 10 minutes (6.47%), implying that higher voltage with shorter exposure time effectively stabilized the matrix potentially through enhanced cross-linking and limited structural damage. CPT induces electroporation and modifies protein

conformation, which can either enhance or compromise the food matrix depending on the treatment severity. Samples with a moderate WAI (water absorption ratio) and well-balanced electroporation, such as those treated at 30 kV, exhibited lower CL, likely due to improved water retention and reduced solute leaching. Interestingly, longer treatments at high voltage (30 kV, 20–30 min) did not further reduce CL significantly, indicating a threshold beyond which additional treatment yields diminishing benefits. Overall, short-duration with high-voltage treatment (30 kV, 10 min) appears most effective in minimizing cooking loss by preserving structural integrity and optimizing water retention capacity.<sup>43</sup> MAR showed a minimal  $\Delta E$  of  $2.16 \pm 0.30$ , reduced CT of  $22.16 \pm 0.37$  min, low CL of  $6.62 \pm 0.28\%$ , WAI of  $4.52 \pm 0.27$  g g<sup>-1</sup>, WAR of  $4.31 \pm 0.26$ , and a WSI of  $2.16 \pm 0.30$  g per 100 g, at high-intensity CPT (30 kV for 30 minutes) confirming that the physical structure becomes more compact and less reactive. These transformations suggest that a dense oxidized surface layer may be formed, reducing the material's ability to absorb or dissolve in water while enhancing its thermal processing efficiency.<sup>48</sup> In conclusion, CPT offers a versatile non-thermal approach to modify the structural and functional properties of MAR. Its impact depends heavily on the treatment intensity and duration. Manufacturers can achieve desired properties such as improved cooking performance, water solubility, or storage stability by carefully tuning these parameters. Molecular-level studies using analytical tools like FTIR, SEM, DSC, and XRD are needed to better understand the mechanisms by which plasma–biopolymer interactions drive these transformations.

### 3.2. Textural analysis

The textural characteristics of cold plasma-treated and untreated millet-based analogue rice (MAR) are presented in Table 2. The treatment with cold plasma resulted in statistically significant changes in both hardness and gumminess, while no significant alterations were observed in springiness and cohesiveness. Specifically, the hardness of MAR increased from  $6.41 \pm 0.141$  N in the untreated sample to  $9.24 \pm 0.142$  N in the treated sample, representing a significant difference ( $p < 0.01$ ,  $t = 14.123$ ). Similarly, gumminess increased from  $2.82 \pm 0.09$  N to  $4.24 \pm 0.195$  N ( $p < 0.01$ ,  $t = 6.478$ ). In contrast, springiness and cohesiveness values remained statistically unchanged with  $t$ -values of 0.296 and 0.154, respectively.<sup>31</sup> These results suggest that cold plasma treatment enhances the firmness and mechanical resistance of millet-based analogue rice. The observed increase in hardness is likely due to plasma-induced modifications in the starch–protein matrix. Cold plasma generates reactive oxygen and nitrogen species (RONS) such as  $\text{-OH}$ ,  $\text{O}_3$ , and  $\text{NO}^+$ , which may initiate oxidative cross-linking between starch and protein chains. This results in a denser and more compact microstructure reducing the material's ability to deform under mechanical stress.<sup>20</sup> Additionally, plasma treatment may lead to partial dehydration of the surface or internal matrix, which can further increase firmness by reducing moisture-mediated plasticization.<sup>40</sup> The increase in gumminess, derived from the product of hardness and



Table 2 Textural properties of cold plasma untreated and treated millet-based analogue rice<sup>a</sup>

Parameters	Untreated MAR	Cold plasma treated MAR	t-Value
Hardness (N)	6.41 ± 0.141 <sup>b</sup>	9.24 ± 0.142 <sup>a</sup>	14.123**
Gumminess (N)	2.82 ± 0.099 <sup>b</sup>	4.24 ± 0.195 <sup>a</sup>	6.478**
Springiness (mm)	0.63 ± 0.174 <sup>a</sup>	0.7 ± 0.159 <sup>a</sup>	0.296 <sup>NS</sup>
Cohesiveness	0.44 ± 0.071 <sup>a</sup>	0.46 ± 0.108 <sup>a</sup>	0.154 <sup>NS</sup>

<sup>a</sup> Results are expressed as mean ± SD ( $n = 3$ ). Values in the same row with different letters are significantly different at  $p < 0.05$  (\*\* denotes high significance and <sup>NS</sup> denotes no significance).

cohesiveness, supports the notion that the treated MAR exhibits a more rigid structure. Gumminess is associated with the energy required to disintegrate a semi-solid food and is often enhanced by tighter molecular networking. The presence of plasma-generated free radicals can promote intermolecular bonding and molecular entanglement, particularly among amylose chains leading to increased resistance to breakdown during mastication.<sup>41</sup> Interestingly, springiness and cohesiveness remained unaffected. Springiness refers to the ability of a material to regain its original shape after compression, while cohesiveness measures the internal bonding strength of the material. The lack of significant changes in these parameters suggests that the elastic properties and internal matrix integrity of MAR were preserved. This could be attributed to the fact that cold plasma primarily affects the outer layers or surface interactions of grains, rather than penetrating deep enough to modify internal viscoelastic behaviour in short treatment durations.<sup>49</sup> Additionally, these properties are highly moisture-dependent and may not respond significantly to structural rearrangements unless the hydration level or molecular mobility is drastically altered.<sup>43</sup>

Overall, these findings emphasize the potential of cold plasma treatment as a novel non-thermal technology to improve the textural attributes of millet-based analogue rice. The enhancement of hardness and gumminess could improve consumer perception of product quality, especially in applications where firmness and chewiness are desirable. Moreover, springiness and cohesiveness remain stable, which indicate that the overall structural resilience and product integrity are retained. This balance between modification and preservation is crucial for maintaining product appeal and functionality. Future research should investigate the long-term stability of these textural changes as well as explore potential impacts on other quality parameters such as flavour, aroma, and nutritional composition. The understanding on how cold plasma interacts with specific starch and protein fractions at the molecular level could further refine its application in grain processing and analogue food design.

### 3.3. Rheological properties

The viscoelastic behaviour of cold plasma-treated and untreated MAR was evaluated using dynamic rheological parameters including storage modulus ( $G'$ ), loss modulus ( $G''$ ), shear stress, and viscosity, as shown in Fig. 1. These parameters serve as vital indicators of the material's structural integrity, deformation

behaviour, and functional performance, particularly during cooking and processing. The cold plasma-treated MAR demonstrated significantly higher values for both  $G'$  and  $G''$  compared to the untreated control, indicating a more elastic and mechanically robust network structure.<sup>50,51</sup> The storage modulus ( $G'$ ) reflects the material's ability to store energy in an elastic (recoverable) manner, whereas the loss modulus ( $G''$ ) corresponds to the viscous (non-recoverable) energy dissipation during deformation. The simultaneous elevation of both moduli in the cold plasma-treated samples implies that plasma exposure enhanced both the rigidity and the energy-dissipating capacity of MAR. It resulted in a structure that is more resistant to deformation while maintaining flexibility under mechanical stress.<sup>43</sup> This structural enhancement is likely driven by plasma-generated reactive species (such as ozone, superoxide, and hydroxyl radicals), which can induce oxidative cross-linking of biopolymers primarily starch and proteins within the MAR matrix.<sup>20</sup> Such cross-linking reinforces the internal structure and limits molecular mobility by improving viscoelasticity.

Cold plasma-treated MAR exhibited significantly higher shear stress and viscosity compared to the untreated sample. Shear stress measures the internal resistance of the material to flow or deformation while viscosity indicates its resistance to applied shear forces under a steady-state flow. The increased values for both parameters suggest the development of a denser and more cohesive gel-like matrix that resists breakdown during cooking or mechanical handling.<sup>52</sup> These results are indicative of a modified molecular architecture, where the cold plasma-induced interactions result in greater entanglement and rigidity of the polysaccharide network. The higher viscosity also implies that the treated MAR may form a more stable and cohesive paste during cooking potentially reducing syneresis or undesirable textural breakdown in finished products.<sup>51</sup> These improvements in viscoelastic properties carry significant implications for the cooking performance of MAR. A higher storage modulus typically translates to improved shape retention and reduced cooking-induced disintegration, whereas increased viscosity and shear resistance contribute to a firmer bite. This enhanced chewiness and qualities often associated with consumer-preferred textural attributes in rice-based dishes.<sup>53</sup> The firmer structure of cold plasma-treated MAR not only enhances sensory appeal but also increases tolerance to reheating and extended holding times, further expanding its application in ready-to-eat and convenience foods.<sup>54</sup> Interestingly, the cold plasma treatment improved structural rigidity and resistance to flow but it did not negatively impact the



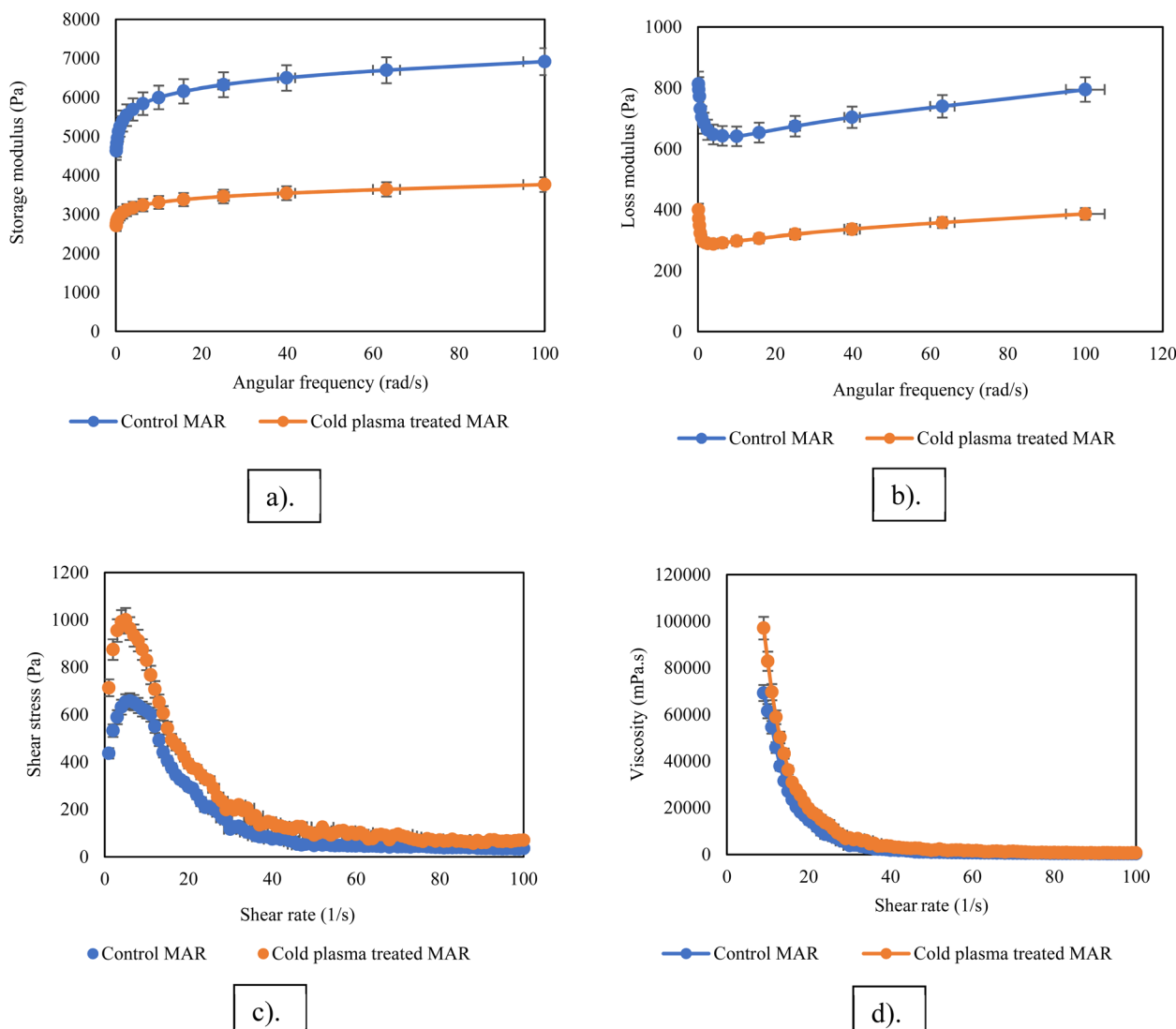


Fig. 1 Rheological properties of untreated and cold plasma-treated millet-based analogue rice. (a) Storage modulus ( $G'$ ) vs. angular frequency. (b) Loss modulus ( $G''$ ) vs. angular frequency. (c) Shear stress vs. shear rate. (d) Viscosity vs. shear rate.

processability of the MAR. This suggests that plasma parameters were within a threshold that promotes structural reinforcement without inducing excessive brittleness or brittleness-related defects. The ability to fine-tune viscoelastic properties without compromising processability highlights the versatility of cold plasma as a tool for texture enhancement in cereal-based analogues.

In conclusion, cold plasma treatment significantly improves the viscoelastic properties of millet-based analogue rice by enhancing its storage and loss moduli, shear stress, and viscosity. These changes are attributed to molecular-level modifications involving oxidative cross-linking and structural tightening of the starch–protein matrix. The resulting improvements in texture, chewiness, and cooking performance suggest that cold plasma-treated MAR could serve as a promising alternative to conventional rice particularly in applications requiring enhanced mechanical and textural stability. Future

studies should focus on optimizing treatment parameters and exploring the long-term effects on sensory attributes, shelf life, and nutritional retention to fully leverage cold plasma's potential in food processing.

### 3.4. Pasting properties

The pasting properties of untreated and cold plasma-treated millet-based analogue rice (MAR) are presented in Table 3. Cold plasma treatment resulted in a significant reduction in all pasting parameters that include peak viscosity, breakdown viscosity, final viscosity, holding strength, and setback values compared to those of the untreated MAR.<sup>55</sup> Specifically, peak viscosity decreased substantially from  $467.8 \pm 0.127$  cP in the untreated sample to  $285.5 \pm 0.123$  cP in the treated sample ( $P < 0.01$ ,  $t = 1028.293$ ). Breakdown viscosity also declined from  $283 \pm 0.216$  cP to  $243.7 \pm 0.104$  cP ( $P < 0.01$ ,  $t = 163.144$ ), and the final viscosity dropped from 486.1 cP to 129.2 cP ( $P < 0.01$ ).



Table 3 Pasting properties of cold plasma untreated and treated millet-based analogue rice<sup>a</sup>

Parameters	Untreated MAR	Cold plasma treated MAR	t-Value
Peak viscosity (cP)	467.8 ± 0.127 <sup>a</sup>	285.5 ± 0.123 <sup>b</sup>	1028.293**
Breakdown viscosity (cP)	283 ± 0.216 <sup>a</sup>	243.7 ± 0.104 <sup>b</sup>	163.144**
Setback from trough (cP)	203.1 ± 0.123 <sup>a</sup>	-114.6 ± 0.144 <sup>b</sup>	1667.161**
Setback from peak (cP)	-18.32 ± 0.171 <sup>b</sup>	156.3 ± 0.097 <sup>a</sup>	883.009**
Final viscosity (cP)	486.1 ± 0.198 <sup>a</sup>	129.2 ± 0.118 <sup>b</sup>	1542.116**
Pasting temperature (°C)	78 ± 0.201 <sup>a</sup>	60.8 ± 0.104 <sup>b</sup>	75.777**
Peak temperature (°C)	95 ± 0.153 <sup>a</sup>	95 ± 0.165 <sup>a</sup>	0.000 <sup>NS</sup>
Peak time (minutes)	4.3 ± 0.307 <sup>a</sup>	1.03 ± 0.164 <sup>b</sup>	9.385**
Holding strength (cP)	184.8 ± 0.230 <sup>a</sup>	41.72 ± 0.199 <sup>b</sup>	469.220**

<sup>a</sup> Results are expressed as mean ± SD ( $n = 3$ ). Values in the same row with different letters are significantly different at  $p < 0.05$  (\* denotes significance and \*\* denotes high significance).

Additionally, the holding strength significantly decreased from 184.8 cP to 41.72 cP ( $P < 0.01$ ) while the setback from the peak and trough values turned negative in the treated sample, indicating major changes in retrogradation behaviour. The pasting temperature declined from 78 °C to 60.8 °C although the peak temperature remained consistent at 95 °C in both cases. The peak time was significantly reduced from 4.3 minutes to 1.03 minutes ( $t = 9.385$ ,  $P < 0.01$ ).<sup>39,43</sup> These alterations in pasting behaviour reveal that cold plasma treatment significantly affects the gelatinization characteristics of starch in MAR. The reduction in peak and final viscosities is indicative of structural disruption in starch granules, likely caused by oxidative cleavage of glycosidic linkages and depolymerization of amylose and amylopectin chains. Cold plasma generates reactive oxygen and nitrogen species (RONS) such as O<sub>3</sub>, -OH, and NO<sup>+</sup>, which can modify starch molecules through oxidation and radical-mediated chain scission.<sup>20,31</sup> These modifications weaken the granules' ability to swell and retain water, lowering their capacity to develop high viscosities during heating.

The observed decrease in breakdown viscosity and holding strength implies a reduction in starch paste stability under thermal and mechanical stress. Typically, breakdown viscosity is associated with the collapse of swollen starch granules during shear and heat exposure. Cold plasma-treated MAR with its structurally compromised granules is less stable to maintain paste integrity under such conditions.<sup>39</sup> The reduction in holding strength suggests diminished gel stability after obtaining peak viscosity with a lower capacity to resist breakdown during continued heating. Moreover, the negative setback from both the peak and trough values in the treated samples points to reduced retrogradation, which is the tendency of gelatinized starch to reassociate and crystallize upon cooling. This outcome is beneficial in certain food applications where softer textures or lower staling rates are preferred. The reduced setback may be attributed to the disruption of amylose chains, which play a central role in retrogradation.<sup>43</sup> Less chain alignment and hydrogen bonding upon cooling result in a softer less cohesive gel which may enhance mouthfeel but could also reduce structural firmness in certain applications. The significant decrease in pasting temperature (from 78 °C to 60.8 °C) indicates that cold plasma treatment makes starch granules

more readily gelatinizable, requiring lower energy input for the gelatinization process. This could be advantageous in improving cooking efficiency. The reduction in peak time from 4.3 minutes to 1.03 minutes further supports the hypothesis that starch granules in the treated MAR absorb water and undergo swelling more rapidly due to partial pre-gelatinization or molecular rearrangement caused by plasma exposure.<sup>51</sup> The unchanged peak temperature (95 °C) suggests that while cold plasma affects the initiation of gelatinization, it does not alter the final temperature required to complete the process.

In summary, cold plasma treatment significantly modifies the pasting properties of millet-based analogue rice leading to reduced viscosity, lowered gelatinization temperature, decreased thermal and shear stability, and suppressed retrogradation. These physicochemical changes are primarily driven by oxidative degradation and reorganization of starch molecules under plasma-generated RONS. These changes can enhance cooking efficiency and yield softer textures. They may also affect product structure, shelf life, and consumer acceptability, depending on the application. Therefore, it is essential to optimize cold plasma parameters to balance functionality and quality. Further studies should explore the implications of these modifications on the nutritional profile, sensory perception, and digestibility of MAR-based foods.

### 3.5. FTIR analysis

Fourier-transform infrared (FTIR) spectroscopy was employed to elucidate the structural modifications in MAR induced by cold plasma treatment. The comparative FTIR spectra of untreated and plasma-treated MAR (Fig. 2) reveal significant alterations in both peak positions and intensities, suggesting extensive molecular-level transformations.<sup>43</sup> These changes reflect the reorganization or degradation of specific chemical bonds and functional groups within the biopolymeric matrix of MAR driven by reactive species generated during plasma exposure. In the untreated MAR, characteristic peaks were observed at 2980 cm<sup>-1</sup>, 1146 cm<sup>-1</sup>, and 965 cm<sup>-1</sup>, corresponding respectively to C-H stretching vibrations of aliphatic chains, C-O-C stretching in carbohydrate backbones and vibrations associated with glycosidic linkages. These bands are typical signatures of native polysaccharide and starch structures. The



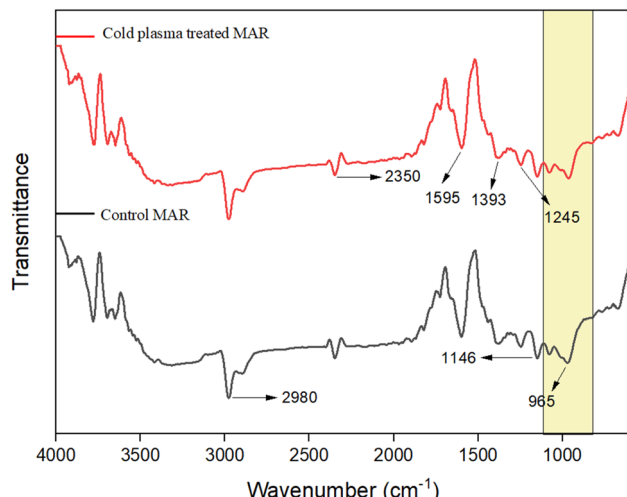


Fig. 2 FTIR spectra of untreated and cold plasma treated millet-based analogue rice.

965  $\text{cm}^{-1}$  band, in particular, is indicative of the  $\alpha$ -(1,4) glycosidic bonds that underpin starch granule integrity. The intensity and sharpness of these bands suggest a well-ordered and compact polysaccharide matrix in untreated MAR. Upon cold plasma treatment, several new absorption peaks appeared at 2350  $\text{cm}^{-1}$ , 1595  $\text{cm}^{-1}$ , 1393  $\text{cm}^{-1}$ , and 1245  $\text{cm}^{-1}$ , consistent with oxidative modifications and structural perturbations. The 2350  $\text{cm}^{-1}$  band is typically attributed to asymmetric stretching of  $\text{CO}_2$  or carbonyl-containing degradation products, reflecting oxidative cleavage of carbon backbones likely mediated by plasma-generated ozone, singlet oxygen, or hydroxyl radicals. These species can initiate  $\beta$ -scission or radical recombination fragmenting polysaccharide chains and introducing carbonyl or carboxyl fractions.

The emergence of the 1595  $\text{cm}^{-1}$  and 1393  $\text{cm}^{-1}$  peaks may correspond to asymmetric and symmetric stretching of  $\text{COO}^-$  groups, respectively, suggesting the formation of carboxylate functionalities. These modifications could arise from oxidative deamination or decarboxylation of amino acid side chains or oxidative fragmentation of fatty acid components in lipoprotein complexes. These modifications are indicative of partial oxidation of proteins and lipids potentially altering their secondary structure and influencing their interactions within the food matrix. Importantly, the 1245  $\text{cm}^{-1}$  peak denotes C–O stretching vibrations often associated with changes in polysaccharide conformation and branching. This shift may reflect the cleavage of native glycosidic bonds and the formation of new ether or ester linkages, suggesting that plasma treatment induces polymer rearrangement or partial depolymerization. These modifications can disrupt hydrogen bonding, polymer chain mobility, and alter hydration properties. The reduction in the intensity of the 1146  $\text{cm}^{-1}$  and 965  $\text{cm}^{-1}$  peaks in the treated samples further supports the hypothesis of glycosidic bond disruption and loss of the ordered starch structure. This degradation weakens the polymer network increasing water accessibility to hydroxyl groups and amorphous regions by enhancing water absorption capacity (WAC). This mechanism is consistent with

the observed improvement in cooking properties such as reduced cooking time and improved softness, which are critical for consumer acceptability.<sup>27</sup>

The oxidative modifications and structural loosening may confer greater resistance to enzymatic hydrolysis as steric hindrance and altered substrate specificity can reduce susceptibility to digestive enzymes. This could contribute to a lower glycaemic response and extended satiety, positioning plasma-treated MAR as a functional ingredient with potential health benefits. Moreover, cold plasma treatment may improve nutrient bioavailability by unmasking bound or encapsulated micronutrients and enhancing protein digestibility through partial unfolding or denaturation. These effects can be linked to the increased surface area and reduced crystallinity, which promote interfacial interactions with digestive enzymes and enhanced solubility. In summary, FTIR spectral analysis confirms that cold plasma induces targeted chemical and structural modifications in MAR *via* oxidative mechanisms. These changes disrupt native polysaccharide and protein matrices leading to enhanced functional properties such as improved water absorption, modified cooking behaviour, and potential nutritional advantages. The treatment appears to modify key molecular interactions such as hydrogen bonding, van der Waals forces, and covalent linkages within the MAR matrix, contributing to changes in physicochemical behaviour. These findings highlight the utility of cold plasma as a non-thermal, green technology for structurally tuning carbohydrate-based food materials. However, future studies should focus on elucidating the exact reaction pathways of plasma-induced modifications to assess the long-term stability and sensory impact, and establish the safety profile for widespread food application.<sup>52</sup>

### 3.6. X-ray diffraction analysis

The X-ray diffraction (XRD) patterns of untreated and cold plasma-treated millet-based analogue rice (MAR) (Fig. 3) reveal

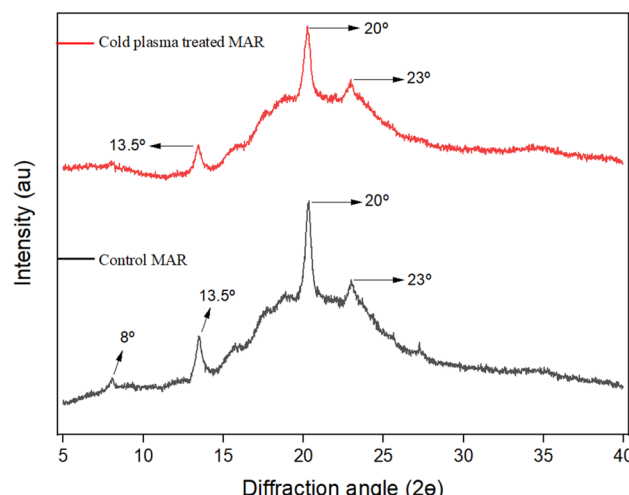


Fig. 3 X-ray diffraction pattern of untreated and cold plasma treated dried millet-based analogue rice.



marked differences in crystallinity, indicating that cold plasma treatment significantly alters the molecular organization of starch granules. The untreated MAR exhibited broad diffraction peaks, particularly at  $2\theta$  angles of  $8^\circ$ ,  $13.5^\circ$ ,  $20^\circ$ , and  $23^\circ$ , characteristic of a less ordered partially amorphous starch structure. In contrast, the cold plasma-treated MAR displayed sharper and more intense peaks, especially at  $2\theta = 13.5^\circ$ ,  $20^\circ$ , and  $23^\circ$  consistent with a polymorphic starch pattern.<sup>27</sup> The increased sharpness following cold plasma treatment suggests a transition toward a more ordered molecular arrangement within the starch granules. This likely arises from plasma-induced cross-linking and molecular reorientation of starch chains, particularly the linear amylose and branched amylopectin segments. During cold plasma exposure, high-energy reactive species (e.g.,  $O^+$ ,  $N^+$ , and excited-state radicals) interact with the starch matrix promoting partial depolymerization of amorphous regions. This interaction simultaneously induces realignment and tighter packing of polymer chains in crystalline domains.<sup>20</sup> This reorganization enhances hydrogen bonding and van der Waals interactions between adjacent helices of amylopectin leading to increased double helical order and crystalline lamellae formation.<sup>56</sup>

The shift from broad, low-intensity peaks in the untreated MAR to more defined higher-intensity peaks in the treated sample underscores the formation of stable and ordered crystallites. Cold plasma treatment appears to facilitate the development of orthorhombic-type unit cells typical of starch where the helices are densely packed and well-aligned. This transformation implies improved granule integrity and reduced porosity translating into enhanced resistance to swelling and

enzymatic degradation.<sup>57</sup> This molecular reordering often correlates with improved mechanical strength, reduced water absorption, and better resistance to retrogradation, which are the key factors in maintaining textural stability during storage and processing. Structurally, the transition from amorphous to a semi-crystalline state in MAR has multiple implications. Crystalline domains are less hydrophilic and more thermally stable, thus lowering the tendency of starch to undergo retrogradation or form a sticky gel upon cooling.<sup>43</sup> In practical terms, this contributes to a firmer, less adhesive texture and better cooking quality parameters that define consumer acceptability in rice analogues. The retention of starch granule morphology enhances the mechanical strength and chewiness of the final product improving its sensory profile and mimicking the textural cues of traditional rice. A previous study has also demonstrated that plasma processing can result in surface restructuring of starch granules without compromising the granule size or integrity, which supports the observation of improved granule alignment in the present study.<sup>20</sup> The oxidative and energetic environment during cold plasma treatment likely facilitates subtle molecular rearrangements at both the surface and interior of the granules, reinforcing crystalline lamellae while limiting the degradation of internal structures.<sup>27</sup>

The relative crystallinity, which reflects the molecular order within starch granules, was notably higher in the control MAR (25.32%) than in the cold plasma-treated sample (19.41%). This decline in crystallinity suggests significant disruption of the starch granule structure following plasma exposure.<sup>58</sup> Such changes likely result from the action of reactive plasma species, especially reactive oxygen species (ROS) like atomic oxygen ( $O^-$ ),

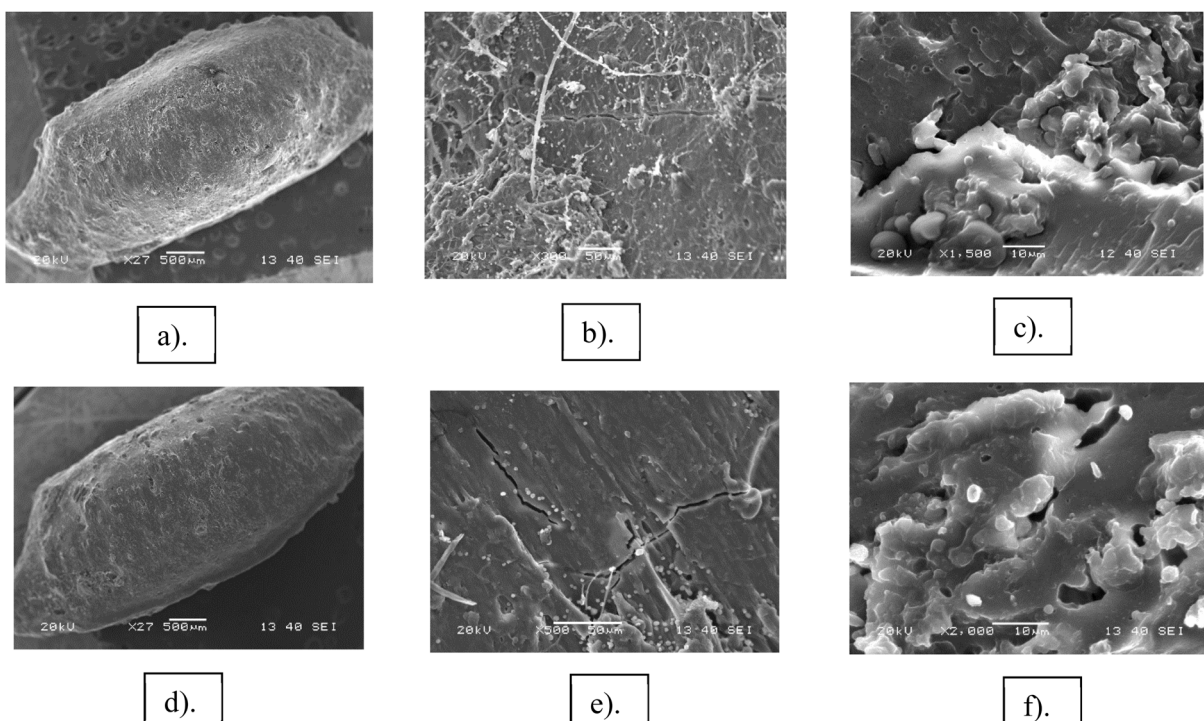


Fig. 4 SEM analysis of untreated (a – surface, b and c – cross sectional view) and cold plasma treated millet-based analogue rice (d – surface, e and f – cross sectional view).

ozone ( $O_3$ ), and hydroxyl radicals ( $-OH$ ). These reactive molecules interfere with the hydrogen bonding that maintains the amylopectin double helices in crystalline regions, causing partial unwinding and a loss of ordered arrangement. In addition, oxidation of hydroxyl groups weakens intermolecular interactions, further destabilizing the crystalline–amorphous lamellar arrangement. Cleavage of glycosidic bonds by plasma species, particularly in the amorphous regions, leads to chain scission, fragmentation, and depolymerization of amylopectin and amylose molecules. Physical effects such as surface erosion and etching from bombardment of plasma species also contribute to increased amorphous character, which is evident from the SEM images (Fig. 4). These results are in line with previous reports on rice starch, where  $R_c$  decreased from 43.06% (untreated starch) to 37.47% following cold plasma treatment, mainly due to depolymerization of starch molecules caused by the reactive plasma species.<sup>59</sup> Similar results of reduced relative crystallinity were also reported in ref. 58 on potato starch and ref. 60 on red adzuki bean starch.

These results suggest that cold plasma-treated MAR may be more resistant to physical breakdown and structural collapse during thermal processing or storage. The presence of well-defined crystalline domains also supports long-term shelf stability and reduced susceptibility to microbial or oxidative deterioration. This translates into improved functionality in ready-to-eat, instant, or retort rice analogue applications from a commercial perspective. In conclusion, cold plasma treatment induces structural reorganization at the molecular level promoting alignment and crystallization of starch polymers within MAR. The enhanced diffraction intensity and peak resolution observed *via* XRD confirm the transition to a more crystalline state which correlates with improved textural integrity, mechanical strength, and storage stability. These changes are driven by increased hydrogen bonding, tighter helical packing, and enhanced molecular ordering due to the plasma-generated reactive environment. As a result, cold plasma-treated MAR presents a promising strategy to enhance the physicochemical properties of millet-based rice analogues in food processing applications.

### 3.7. SEM analysis

The scanning electron microscopy (SEM) images of millet-based analogue rice (MAR) before and after cold plasma treatment (Fig. 4) reveal substantial alterations in the surface morphology and internal microstructure, underscoring the structural impact of the cold plasma process. The untreated MAR exhibited a smooth and continuous surface with minimal surface disruptions or pore formation. This morphology is characteristic of starch-based materials with intact granule organization and low surface energy, indicative of minimal physical processing. In contrast, the cold plasma-treated MAR showed a significantly rougher and more porous surface topology characterized by microfractures, pits, and increased surface irregularity. This change is likely due to rapid moisture desorption and effects induced by the highly energetic plasma environment. During treatment, reactive oxygen and nitrogen

species (RONS) such as ozone ( $O_3$ ), singlet oxygen ( $^1O_2$ ), and nitrogen radicals ( $NO^+$  and  $N_2^+$ ) interact with the surface starch matrix, leading to localized oxidation, ablation, and breakdown of weaker amorphous regions.<sup>20,61</sup> This results in microstructural rearrangements and an increase in the free volume at the surface. The observed increase in porosity and surface roughness may have important functional implications especially for water–matrix interactions. A rougher surface increases the available surface area for water contact and capillary uptake, which enhances water absorption capacity and rehydration rate properties critical for the design of instant or ready-to-cook formulations.<sup>27</sup> This also supports improved binding with added hydrocolloids or nutrients in multi-component food systems.

The cross-sectional SEM analysis reveals additional insights into the internal structural transformations. Untreated MAR displayed loosely packed starch granules consistent with a native or minimally processed starch matrix. These granules appear irregularly distributed with visible inter-granular voids indicative of poor molecular cohesion and limited structural consolidation. In contrast, the cold plasma-treated MAR exhibited a denser and more compact internal network. The starch granules appear more fused with fewer voids and the overall structure is notably more homogeneous. This densification suggests partial gelatinization or restructuring of the internal matrix potentially resulting from localized thermal and oxidative effects during plasma exposure.<sup>47</sup> The molecular mechanism behind this densification likely involves starch depolymerization and recombination where disrupted amylopectin and amylose chains realign into a tighter and entangled matrix. Additionally, cold plasma may induce limited cross-linking of hydroxyl groups on glucose residues enhancing the cohesion and rigidity of the internal structure.<sup>43</sup> This reorganization stabilizes the matrix, reducing free volume and increasing structural resistance to mechanical stress. The increased internal density enhances the mechanical strength of the MAR granules, reducing brittleness and breakage during transportation, handling, and storage. This structural reinforcement is particularly beneficial for dried or pre-packaged products that are subjected to mechanical loads. The dual effects of surface porosity and internal densification indicate that cold plasma treatment can simultaneously optimize both hydration behaviour and mechanical integrity, which are often opposing requirements in food design. Porous structures usually facilitate hydration but compromise structural stability. However, in this case, the synergistic effects of surface modification and internal consolidation provide a balance between rapid water uptake and textural durability.<sup>52</sup>

The improvements in hydration and mechanical properties also imply potential benefits in sensorial attributes such as chewiness and firmness, enhancing the overall consumer acceptability of MAR. The enhanced rehydration rate may allow for reduced cooking times, contributing to the convenience and energy efficiency of MAR-based meals. In conclusion, the SEM analysis confirms that cold plasma treatment induces multi-scale structural modifications in MAR ranging from increased surface porosity to enhanced internal granule packing. These



morphological changes are driven by plasma-induced physico-chemical interactions including surface modification, molecular fragmentation, and partial thermal restructuring. These alterations translate into improved water absorption, rehydration kinetics, and mechanical resilience making cold plasma-treated MAR a promising candidate for functional, fast-cooking, and shelf-stable food products. Future work should aim to optimize plasma exposure parameters (e.g., gas composition, treatment time, and power density) to tailor porosity and structural integrity for specific food applications.

### 3.8. Elemental analysis

Table 4 illustrates the statistically significant differences in elemental concentrations (in ppm) between the control and cold plasma-treated millet-based analogue rice (MAR). These findings highlight the ability of cold plasma to modify the mineral composition potentially improving the nutritional quality of MAR through alterations in surface chemistry, porosity, and matrix reactivity. Cold plasma-treated MAR showed a slight but statistically significant reduction in sodium content ( $111.19 \pm 0.480$  ppm) compared to that of the control ( $112.35 \pm 0.493$  ppm), possibly due to plasma-induced ionic exchange or surface desorption effects. In contrast, macro elements such as magnesium, phosphorus, potassium, and calcium exhibited dramatic increases in concentration. Specifically, magnesium content rose from  $262.10 \pm 0.376$  ppm in the control to  $633.72 \pm 0.301$  ppm after treatment which is a highly significant enhancement. Similarly, phosphorus increased from  $555.75 \pm 0.560$  ppm to  $1678.56 \pm 0.382$  ppm, and potassium from  $48.01 \pm 0.396$  ppm to  $244.95 \pm 0.382$  ppm. Calcium achieved an 18-fold increase from  $5.43 \pm 0.345$  ppm to  $99.88 \pm 0.405$  ppm. These substantial changes suggest that cold plasma enhances the surface reactivity or accessibility of mineral-binding sites on starch and protein matrices.<sup>43</sup> The treatment likely promotes surface oxidation and microcrack formation as confirmed by SEM, increasing porosity and thereby exposing internal mineral-rich domains. Reactive species such as oxygen radicals and ozone can modify the structure of cell wall

components breaking down bound complexes and releasing chelated minerals enhancing their extractability and potential bioavailability.<sup>20,62</sup>

Among trace elements, cold plasma treatment also significantly increased concentrations of chromium (from  $1.00 \pm 0.267$  to  $3.30 \pm 0.264$  ppm), manganese ( $1.71 \pm 0.309$  to  $6.19 \pm 0.329$  ppm), iron ( $83.92 \pm 0.368$  to  $257.03 \pm 0.312$  ppm), copper, and zinc. These elements are essential cofactors for enzymatic processes related to metabolism, redox balance, and immune response.<sup>63</sup> The elevated concentrations of these trace minerals suggest that cold plasma can enhance the mineral nutritional profile of MAR, potentially contributing to better human health outcomes, especially in populations dependent on staple cereals. For certain elements like nickel and molybdenum, there were no statistically significant changes between the control and treated samples, indicating selective effects of plasma on mineral mobilization. This selectivity may be related to differences in the chemical speciation, oxidation state, or binding affinity of elements within the MAR matrix. For example, elements bound in highly stable organo-metallic complexes may be less responsive to plasma-induced disruption compared to more loosely bound ions.<sup>35,64</sup> Mechanistically, the increase in essential macro- and micro-minerals can be attributed to the modification of matrix hydrophilicity, surface charge, and chemical reactivity. Cold plasma introduces polar functional groups (e.g., -OH, and -COOH) onto the surface of biopolymers such as starch and proteins, which may enhance their cation exchange capacity, facilitating the release or retention of minerals.<sup>61</sup> These physicochemical changes can also influence subsequent mineral analysis by improving digestion efficiency or altering solubility during sample preparation.

The nutritional implications of these enhancements are considerable. The key macro elements like potassium, phosphorus, calcium, and magnesium play essential roles in osmoregulation, bone health, and enzymatic activation. Similarly, trace elements like iron, zinc, manganese, and chromium are crucial for oxygen transport, antioxidant defence, glucose

Table 4 The concentration of different mineral contents in the MAR sample<sup>a</sup>

Parameters	Untreated MAR (ppm)	Cold plasma treated MAR (ppm)	t Value
<sup>23</sup> Na (sodium)	$112.35 \pm 0.493^a$	$111.19 \pm 0.480^b$	$4.121^{**}$
<sup>24</sup> Mg (magnesium)	$262.10 \pm 0.376^b$	$633.72 \pm 0.301^a$	$1886.979^{**}$
<sup>31</sup> P (phosphorus)	$555.75 \pm 0.566^b$	$1678.56 \pm 0.382^a$	$4024.576^{**}$
<sup>39</sup> K (potassium)	$48.01 \pm 0.396^b$	$244.95 \pm 0.382^a$	$876.222^{**}$
<sup>44</sup> Ca (calcium)	$5.43 \pm 0.345^b$	$99.88 \pm 0.405^a$	$434.216^{**}$
<sup>48</sup> Ti (titanium)	$0.15 \pm 0.113^b$	$0.47 \pm 0.219^a$	$3.182^*$
<sup>52</sup> Cr (chromium)	$1.00 \pm 0.276^b$	$3.30 \pm 0.264^a$	$14.675^{**}$
<sup>55</sup> Mn (manganese)	$1.71 \pm 0.309^b$	$6.19 \pm 0.329^a$	$24.255^{**}$
<sup>57</sup> Fe (iron)	$83.92 \pm 0.368^b$	$257.03 \pm 0.312^a$	$877.245^{**}$
<sup>60</sup> Ni (nickel)	$0.15 \pm 0.119^b$	$0.36 \pm 0.249^a$	$1.915^{NS}$
<sup>63</sup> Cu (copper)	$0.37 \pm 0.139^b$	$0.90 \pm 0.229^a$	$4.813^{**}$
<sup>66</sup> Zn (zinc)	$0.80 \pm 0.269^b$	$6.03 \pm 0.305^a$	$31.419^{**}$
<sup>95</sup> Mo (molybdenum)	$0.13 \pm 0.115^b$	$0.42 \pm 0.296^a$	$2.185^{NS}$

<sup>a</sup> Results are expressed as mean  $\pm$  SD ( $n = 3$ ). Values in the same row with different letters are significantly different at  $p < 0.05$  (\*\* denotes high significance and NS denotes non-significant).



metabolism, and numerous enzymatic pathways.<sup>65</sup> Therefore, cold plasma-treated MAR may offer an improved mineral profile, making it a nutritious and functional alternative to conventional rice products, especially in micronutrient-deficient regions. Cold plasma presents an innovative post-harvest technology to improve nutrient density in staple crops. The use of this technology could address micronutrient deficiencies in vulnerable populations, particularly where dietary diversity is limited.<sup>66</sup> However, further research is needed to clarify the mechanisms underlying mineral transformation including the potential effects of plasma gas type, power, duration, and moisture content. Moreover, the long-term stability, bioavailability, and sensory impacts of these mineral changes in MAR require detailed exploration. The elemental analysis confirms that cold plasma treatment induces significant enhancements in both macro- and micro-mineral concentrations in MAR. These changes are likely driven by plasma-induced structural and chemical modifications which increase mineral availability and potentially improve nutritional quality. This suggests that cold plasma technology can be effectively harnessed to enrich staple foods like millet-based rice analogues with essential nutrients contributing to both food security and public health.

## 4. Conclusion

Cold plasma treatment applied using a multipin atmospheric plasma reactor at 10–30 kV for 10–30 minutes significantly enhanced the functional, cooking, and structural properties of millet-based analogue rice (MAR). The strongest effects were observed at 30 kV for 30 minutes, where high levels of RONS induced key molecular changes, including disruption of glycosidic linkages, formation of new carbonyl/carboxyl groups (FTIR), a reduction in relative crystallinity from 25.32% to 19.41% (XRD), and the development of a rough porous surface with micro-fractures (SEM). These structural modifications drove the major findings of the study: improved water absorption and hydration capacity, reduced cooking time, strengthened rheological behaviour, increased textural firmness, enhanced mineral bioavailability (Mg, P, K, Ca, and Fe), and better overall cooking quality that can positively influence sensory attributes. These results confirm that cold plasma is a reproducible, sustainable, non-thermal technology capable of tailoring the starch structure and substantially improving MAR quality and consumer acceptance. Future research should refine plasma dosimetry and treatment parameters, assess long-term storage stability and sensory performance, and conduct comparative and real-food system trials to support industrial-scale deployment and commercialization of cold-plasma-processed, climate-resilient millet-based foods.

## Author contributions

S. Ganga Kishore: conceptualization, investigation, methodology, validation, writing – original draft. Madhuresh Dwivedi: conceptualization, writing – review and editing, supervision. R. Rahul: writing – original draft, formal analysis. J. Deepa: formal

analysis. G. Jeevarathinam: conceptualization, writing – review and editing. K. Kamaleeswari: formal analysis. Gitanjali Jothiprakash: formal analysis. Abinaya Veluswamy: formal analysis.

## Conflicts of interest

The authors declare no conflicts of interest.

## Abbreviations

WAI	Water absorption index
CT	Cooking time
WAR	Water absorption ratio
CL	Cooking loss
WSI	Water solubility index
MAR	Millet based analogue rice

## Data availability

The data that support the findings of this study are available from the corresponding author upon reasonable request.

## References

- 1 C. Sunil, N. N. Gowda, N. Nayak and A. Rawson, Unveiling the effect of processing on bioactive compounds in millets: Implications for health benefits and risks, *Process Biochem.*, 2024, **138**, 79–96, DOI: [10.1016/j.procbio.2024.01.010](https://doi.org/10.1016/j.procbio.2024.01.010).
- 2 R. Muthuvel, S. Jagannathan, N. K. Pariyapurath, R. G. Pachamuthu, M. Mathanmohun and S. Sagadevan, Harnessing Nutritional Powerhouse: Millets and Probiotics in Anticancer Therapy, *Curr. Pharmacol. Rep.*, 2024, **10**, 259–266, DOI: [10.1007/s40495-024-00360-4](https://doi.org/10.1007/s40495-024-00360-4).
- 3 S. M. Singh, T. J. Joshi and P. S. Rao, Technological advancements in millet dehusking and polishing process; an insight into pretreatment methods, machineries and impact on nutritional quality, *Grain Oil Sci. Technol.*, 2024, **7**(3), 186–195, DOI: [10.1016/j.gaost.2024.05.007](https://doi.org/10.1016/j.gaost.2024.05.007).
- 4 A. A. Sabuz, M. R. Rana, T. Ahmed, *et al.*, Health-promoting potential of millet: A review, *Separations*, 2023, **10**, 80, DOI: [10.3390/separations10020080](https://doi.org/10.3390/separations10020080).
- 5 G. Kaur, S. Ahmadzadeh-Hashemi, S. Amir, *et al.*, From Millet to Marvels: An Improved Future Food through Innovative Processing, *Future Foods*, 2024, **9**, 100367, DOI: [10.1016/j.fufo.2024.100367](https://doi.org/10.1016/j.fufo.2024.100367).
- 6 S. Saini, S. Saxena, M. Samtiya, M. Puniya and T. Dhewa, Potential of underutilized millets as Nutri-cereal: an overview, *J. Food Sci. Technol.*, 2021, **58**(12), 4465–4477, DOI: [10.1007/s13197-021-04985-x](https://doi.org/10.1007/s13197-021-04985-x).
- 7 S. Dey, A. Saxena, Y. Kumar, T. Maity and A. Tarafdar, Understanding the antinutritional factors and bioactive compounds of kodo millet (*Paspalum scrobiculatum*) and little millet (*Panicum sumatrense*), *J. Food Qual.*, 2022, **1578448**, DOI: [10.1155/2022/1578448](https://doi.org/10.1155/2022/1578448).
- 8 G. C. Leandro, D. A. Laroque, A. R. Monteiro, B. A. M. Carciofi and G. A. Valencia, Current status and perspectives of starch



powders modified by cold plasma: A review, *J. Polym. Environ.*, 2024, **32**, 510–523, DOI: [10.1007/s10924-023-03027-1](https://doi.org/10.1007/s10924-023-03027-1).

9 R. K. Gupta, P. Guha and P. P. Srivastav, Physical action of nonthermal cold plasma technology for starch modification, *Food Phys.*, 2024, **1**, 100011, DOI: [10.1016/j.foodp.2024.100011](https://doi.org/10.1016/j.foodp.2024.100011).

10 H.-T. Li, W. Zhang, Y. Chen, W. Pan and Y. Bao, Physical modification of high amylose starch using electron beam irradiation and heat moisture treatment: The effect on multi-scale structure and in vitro digestibility, *Food Chem.*, 2023, **424**, 136344, DOI: [10.1016/j.foodchem.2023.136344](https://doi.org/10.1016/j.foodchem.2023.136344).

11 J.-N. Ekumah, X. Han, Q. Liang, *et al.*, Production of Kudzu starch gels with superior mechanical and rheological properties through submerged ethanol exposure and implications for in vitro digestion, *Foods*, 2023, **12**, 3992, DOI: [10.3390/foods12213992](https://doi.org/10.3390/foods12213992).

12 J. Zhang, Y. Liu, M. Liu, *et al.*, Effects of *Lactiplantibacillus plantarum* dy-1 fermentation on multi-scale structure and physicochemical properties of barley starch, *Food Funct.*, 2024, **15**, 1923–1937, DOI: [10.1039/d3fo04395a](https://doi.org/10.1039/d3fo04395a).

13 Z. Yang, C. Xie, Y. Bao, F. Liu, H. Wang and Y. Wang, Oat: Current state and challenges in plant-based food applications, *Trends Food Sci. Technol.*, 2023, **134**, 56–71, DOI: [10.1016/j.tifs.2023.02.017](https://doi.org/10.1016/j.tifs.2023.02.017).

14 G. Hui, P. Zhu and M. Wang, Structure and functional properties of taro starch modified by dry heat treatment, *Int. J. Biol. Macromol.*, 2024, **261**, 129702, DOI: [10.1016/j.ijbiomac.2024.129702](https://doi.org/10.1016/j.ijbiomac.2024.129702).

15 Y. Hu, Y. Zhu, H. Aalim, *et al.*, Cold plasma-assisted pretreatment for fabrication and characterization of rice starch-stearic acid complexes, *Food Biosci.*, 2024, **60**, 104492, DOI: [10.1016/j.fbio.2024.104492](https://doi.org/10.1016/j.fbio.2024.104492).

16 J.-H. Cheng, X. Ai, J. Ma and D.-W. Sun, Effects of cold plasma pretreatment combined with sodium periodate on property enhancement of dialdehyde starch prepared using native maize starch, *Int. J. Biol. Macromol.*, 2024, **267**, 131435, DOI: [10.1016/j.ijbiomac.2024.131435](https://doi.org/10.1016/j.ijbiomac.2024.131435).

17 S. Jaddu, R. C. Pradhan and M. Dwivedi, Effect of multipin atmospheric cold plasma discharge on functional properties of little millet (*Panicum miliare*) flour, *Innovative Food Sci. Emerging Technol.*, 2022, **77**, 102957, DOI: [10.1016/j.ifset.2022.102957](https://doi.org/10.1016/j.ifset.2022.102957).

18 A. Y. Okyere, S. Rajendran and G. A. Annor, Cold plasma technologies: Their effect on starch properties and industrial scale-up for starch modification, *Curr. Res. Food Sci.*, 2022, **5**, 451–463, DOI: [10.1016/j.crfs.2022.02.007](https://doi.org/10.1016/j.crfs.2022.02.007).

19 R. K. Gupta, P. Guha and P. P. Srivastav, Effect of high voltage dielectric barrier discharge (DBD) atmospheric cold plasma treatment on physicochemical and functional properties of taro (*Colocasia esculenta*) starch, *Int. J. Biol. Macromol.*, 2023, **253**, 126772, DOI: [10.1016/j.ijbiomac.2023.126772](https://doi.org/10.1016/j.ijbiomac.2023.126772).

20 R. Thirumdas, A. Trimukhe, R. Deshmukh and U. Annapure, Functional and rheological properties of cold plasma treated rice starch, *Carbohydr. Polym.*, 2017, **157**, 1723–1731, DOI: [10.1016/j.carbpol.2016.11.050](https://doi.org/10.1016/j.carbpol.2016.11.050).

21 T.-Y. Wu, N.-N. Sun and C.-F. Chau, Application of corona electrical discharge plasma on modifying the physicochemical properties of banana starch indigenous to Taiwan, *J. Food Drug Anal.*, 2018, **26**, 244–251, DOI: [10.1016/j.jfda.2017.03.005](https://doi.org/10.1016/j.jfda.2017.03.005).

22 P. Kaur and U. S. Annapure, Effects of pin-to-plate atmospheric cold plasma for modification of pearl millet (*Pennisetum glaucum*) starch, *Food Res. Int.*, 2023, **169**, 112930, DOI: [10.1016/j.foodres.2023.112930](https://doi.org/10.1016/j.foodres.2023.112930).

23 F. Shokrollahi, F. Shahidi, M. J. Varidi, A. Koocheki, F. Sohbatzadeh and A. Motamedzadegan, Effect of atmospheric pressure argon plasma on physicochemical, structural and rheological properties of sorghum starch, *Starch*, 2023, **75**, 2200187, DOI: [10.1002/star.202200187](https://doi.org/10.1002/star.202200187).

24 Z. Cao, X. Li, H. Song, Y. Jie and C. Liu, Effect of intermittent low-pressure radiofrequency helium cold plasma treatments on rice gelatinization, fatty acid, and hygroscopicity, *Foods*, 2024, **13**, 1056, DOI: [10.3390/foods13071056](https://doi.org/10.3390/foods13071056).

25 R. Li, Z. J. Li, N. N. Wu and B. Tan, The effect of cold plasma pretreatment on GABA,  $\gamma$ -oryzanol, phytic acid, phenolics, and antioxidant capacity in brown rice during germination, *Cereal Chem.*, 2023, **100**, 321–332, DOI: [10.1002/cche.10609](https://doi.org/10.1002/cche.10609).

26 Z. Zeng, Y. Wang, G. Xu, L. Zhou, C. Liu and S. Luo, Peroxidase inactivation by cold plasma and its effects on the storage, physicochemical and bioactive properties of brown rice, *Food Biosci.*, 2023, **52**, 102383, DOI: [10.1016/j.fbio.2023.102383](https://doi.org/10.1016/j.fbio.2023.102383).

27 C. Zhou, Y. Zhou, Q. Tang, *et al.*, Impact of argon dielectric barrier discharge cold plasma on the physicochemical and cooking properties of lightly-milled rice, *Innovative Food Sci. Emerging Technol.*, 2024, **92**, 103580, DOI: [10.1016/j.ifset.2024.103580](https://doi.org/10.1016/j.ifset.2024.103580).

28 C. Zhou, Y. Hu, Y. Zhou, *et al.*, Air and argon cold plasma effects on lipolytic enzymes inactivation, physicochemical properties and volatile profiles of lightly-milled rice, *Food Chem.*, 2024, **445**, 138699, DOI: [10.1016/j.foodchem.2024.138699](https://doi.org/10.1016/j.foodchem.2024.138699).

29 S. Bohlooli, Y. Ramezan, F. Esfarjani, H. Hosseini and S. Eskandari, Effect of soaking in plasma-activated liquids (PALs) on heavy metals and other physicochemical properties of contaminated rice, *Food Chem.: X*, 2024, **24**, 101788, DOI: [10.1016/j.fochx.2024.101788](https://doi.org/10.1016/j.fochx.2024.101788).

30 A. Nithya, S. Vishwakarma, C. G. Dalbhagat and H. N. Mishra, Apparent amylose content positively influences the quality of extruded fortified rice kernels, *Carbohydr. Polym.*, 2024, **338**, 122213, DOI: [10.1016/j.carbpol.2024.122213](https://doi.org/10.1016/j.carbpol.2024.122213).

31 G. P. Yadav, C. G. Dalbhagat and H. N. Mishra, Development of instant low glycemic rice using extrusion technology and its characterization, *J. Food Process. Preserv.*, 2021, **45**, e16077, DOI: [10.1111/jfpp.16077](https://doi.org/10.1111/jfpp.16077).

32 L. Wang, Y. Gong, Y. Li and Y. Tian, Structure and properties of soft rice starch, *Int. J. Biol. Macromol.*, 2020, **157**, 10–16, DOI: [10.1016/j.ijbiomac.2020.04.138](https://doi.org/10.1016/j.ijbiomac.2020.04.138).

33 K. Wang, J. Ma, L. Wang, *et al.*, Insight into the relationship between the starch crystalline structure and textural quality

and physicochemical properties of reconstituted rice: Influence of feed moisture content, *Int. J. Biol. Macromol.*, 2024, **280**, 135758.

34 S. Vishwakarma, S. Mandliya, C. G. Dalbhagat, J. Majumdar and H. N. Mishra, Effect of marjoram leaf powder addition on nutritional, rheological, textural, structural, and sensorial properties of extruded rice noodles, *Foods*, 2023, **12**, 1099, DOI: [10.3390/foods12051099](https://doi.org/10.3390/foods12051099).

35 B. Novotnik, T. Zuliani, J. Ščančar and R. Milačić, Content of trace elements and chromium speciation in Neem powder and tea infusions, *J. Trace Elem. Med. Biol.*, 2015, **31**, 98–106, DOI: [10.1016/j.jtemb.2015.04.003](https://doi.org/10.1016/j.jtemb.2015.04.003).

36 N. Misra, S. Kaur, B. K. Tiwari, A. Kaur, N. Singh and P. Cullen, Atmospheric pressure cold plasma (ACP) treatment of wheat flour, *Food Hydrocolloids*, 2015, **44**, 115–121, DOI: [10.1016/j.foodhyd.2014.08.019](https://doi.org/10.1016/j.foodhyd.2014.08.019).

37 B. Surowsky, S. Bußler and O. Schlüter, Cold plasma interactions with food constituents in liquid and solid food matrices, in *Cold Plasma in Food and Agriculture*, Elsevier, 2016, ch. 7, pp. 179–203, DOI: [10.1016/B978-0-12-801365-6.00007-X](https://doi.org/10.1016/B978-0-12-801365-6.00007-X).

38 R. Thirumdas, A. Kothakota, U. Annapure, *et al.*, Plasma activated water (PAW): Chemistry, physico-chemical properties, applications in food and agriculture, *Trends Food Sci. Technol.*, 2018, **77**, 21–31, DOI: [10.1016/j.tifs.2018.05.007](https://doi.org/10.1016/j.tifs.2018.05.007).

39 F. Zhang, Y. Laraib, X. Chai, *et al.*, The effect of reducing agent DTT on pasting, hydration and microstructure properties of foxtail millet, *J. Cereal Sci.*, 2020, **95**, 103044, DOI: [10.1016/j.jcs.2020.103044](https://doi.org/10.1016/j.jcs.2020.103044).

40 S. K. Pankaj, C. Bueno-Ferrer, N. Misra, *et al.*, Applications of cold plasma technology in food packaging, *Trends Food Sci. Technol.*, 2014, **35**, 5–17, DOI: [10.1016/j.tifs.2013.10.009](https://doi.org/10.1016/j.tifs.2013.10.009).

41 C. Khemthong, U. Suttisansanee, S. Chaveanghong, *et al.*, Physico-functional properties, structural, and nutritional characterizations of Hodgsonia heteroclita oilseed cakes, *Sci. Rep.*, 2024, **14**, 19241, DOI: [10.1038/s41598-024-70276-y](https://doi.org/10.1038/s41598-024-70276-y).

42 F. D. L. Almeida, W. F. Gomes, R. S. Cavalcante, *et al.*, Fructooligosaccharides integrity after atmospheric cold plasma and high-pressure processing of a functional orange juice, *Food Res. Int.*, 2017, **102**, 282–290, DOI: [10.1016/j.foodres.2017.09.072](https://doi.org/10.1016/j.foodres.2017.09.072).

43 S. G. Kishore, M. Dwivedi, C. G. Dalbhagat, *et al.*, Development of Extruded Millet Analogue Rice: A Comparison of Rheological, Structural, Physicochemical, and Cooking Properties with Conventional Rice, *ACS Food Sci. Technol.*, 2024, **4**(10), 2504–2516, DOI: [10.1021/acsfoodscitech.4c00629](https://doi.org/10.1021/acsfoodscitech.4c00629).

44 S. Wang, Y. Liu, Y. Zhang, *et al.*, Processing sheep milk by cold plasma technology: Impacts on the microbial inactivation, physicochemical characteristics, and protein structure, *LWT*, 2022, **153**, 112573, DOI: [10.1016/j.lwt.2021.112573](https://doi.org/10.1016/j.lwt.2021.112573).

45 K. Karthik, B. D. Rao, A. Das, *et al.*, Personalized Kodo Millet Rice Analogue (KMRA): Formulation, nutritional evaluation, and optimization, *Future Foods*, 2024, **10**, 100389, DOI: [10.1016/j.fufo.2024.100389](https://doi.org/10.1016/j.fufo.2024.100389).

46 F. Ge, Y. Sun, C. Yang, *et al.*, Exploring the relationship between starch structure and physicochemical properties: The impact of extrusion on highland barley flour, *Food Res. Int.*, 2024, **183**, 114226, DOI: [10.1016/j.foodres.2024.114226](https://doi.org/10.1016/j.foodres.2024.114226).

47 J. Liu, R. Wang, Z. Chen and X. Li, Effect of cold plasma treatment on cooking, thermomechanical and surface structural properties of Chinese milled rice, *Food Bioprocess Technol.*, 2021, **14**, 866–886, DOI: [10.1007/s11947-021-02614-1](https://doi.org/10.1007/s11947-021-02614-1).

48 R. Pandiselvam, S. Mitharwal, P. Rani, *et al.*, The influence of non-thermal technologies on color pigments of food materials: An updated review, *Curr. Res. Food Sci.*, 2023, **6**, 100529, DOI: [10.1016/j.crfcs.2023.100529](https://doi.org/10.1016/j.crfcs.2023.100529).

49 G. Scott and J. M. Awika, Effect of protein–starch interactions on starch retrogradation and implications for food product quality, *Compr. Rev. Food Sci. Food Saf.*, 2023, **22**, 2081–2111, DOI: [10.1111/1541-4337.13141](https://doi.org/10.1111/1541-4337.13141).

50 X. Ge, H. Shen, X. Sun, *et al.*, Insight into the improving effect on multi-scale structure, physicochemical and rheology properties of granular cold water soluble rice starch by dielectric barrier discharge cold plasma processing, *Food Hydrocolloids*, 2022, **130**, 107732, DOI: [10.1016/j.foodhyd.2022.107732](https://doi.org/10.1016/j.foodhyd.2022.107732).

51 P. Kaur and U. S. Annapure, Understanding the atmospheric cold plasma-induced modification of finger millet (*Eleusine coracana*) starch and its related mechanisms, *Int. J. Biol. Macromol.*, 2024, **268**, 131615, DOI: [10.1016/j.ijbiomac.2024.131615](https://doi.org/10.1016/j.ijbiomac.2024.131615).

52 A. K. Anal, R. Singh, D. L. Rice, *et al.*, Millets as supergrain: A holistic approach for sustainable and healthy food product production, *Sustainable Food Technol.*, 2024, **2**(4), 908–925, DOI: [10.1039/D4FB00047A](https://doi.org/10.1039/D4FB00047A).

53 L. Muhammad, S. Y. Yeoh and M. M. Shaban, Hydrocolloids in Rice Noodle Production: Enhancing Texture, Cooking Quality, and Sustainability in Gluten-Free Formulations: A Review, *J. Food Innovation Nutr. Environ. Sci.*, 2024, **1**(1), 30–46, DOI: [10.70851/qdw8d910](https://doi.org/10.70851/qdw8d910).

54 T. Dapčević-Hadnadev, J. Tomić, D. Škrobot, B. Šarić and M. Hadnadev, Processing strategies to improve the breadmaking potential of whole-grain wheat and non-wheat flours, *Discover Food*, 2022, **2**, 11, DOI: [10.1007/s44187-022-00012-w](https://doi.org/10.1007/s44187-022-00012-w).

55 C. Collar, Significance of heat-moisture treatment conditions on the pasting and gelling behaviour of various starch-rich cereal and pseudocereal flours, *Food Sci. Technol. Int.*, 2017, **23**, 623–636, DOI: [10.1177/1082013217714671](https://doi.org/10.1177/1082013217714671).

56 Y. Wu, Y. Liu, Y. Jia, C.-H. Feng, F. Ren and H. Liu, Research progress on the regulation of starch-polyphenol interactions in food processing, *Int. J. Biol. Macromol.*, 2024, 135257, DOI: [10.1016/j.ijbiomac.2024.135257](https://doi.org/10.1016/j.ijbiomac.2024.135257).

57 H. Li, M. A. Fitzgerald, S. Prakash, T. M. Nicholson and R. G. Gilbert, The molecular structural features controlling stickiness in cooked rice, a major palatability determinant, *Sci. Rep.*, 2017, **7**, 43713, DOI: [10.1038/srep43713](https://doi.org/10.1038/srep43713).

58 Z. Liu, X. Zhang, Z. Li, Y. Lu, Z. Xu, Q. Shen and Y. Chi, New insights into cold plasma-induced starch modification: A



comparative analysis of microstructure and physicochemical properties in A-type and B-type starches, *Food Chem.*, 2025, **478**, 143708, DOI: [10.1016/j.foodchem.2025.143708](https://doi.org/10.1016/j.foodchem.2025.143708).

59 R. Thirumdas, A. Trimukhe, R. R. Deshmukh and U. S. Annapure, Functional and rheological properties of cold plasma treated rice starch, *Carbohydr. Polym.*, 2017, **157**, 1723–1731, DOI: [10.1016/j.carbpol.2016.11.050](https://doi.org/10.1016/j.carbpol.2016.11.050).

60 X. Ge, H. Shen, C. Su, B. Zhang, Q. Zhang, H. Jiang and W. Li, The improving effects of cold plasma on multi-scale structure, physicochemical and digestive properties of dry heated red adzuki bean starch, *Food Chem.*, 2021, **349**, 129159, DOI: [10.1016/j.foodchem.2021.129159](https://doi.org/10.1016/j.foodchem.2021.129159).

61 S. Gao, H. Zhang, J. Pei, *et al.*, High-voltage and short-time dielectric barrier discharge plasma treatment affects structural and digestive properties of Tartary buckwheat starch, *Int. J. Biol. Macromol.*, 2022, **213**, 268–278, DOI: [10.1016/j.ijbiomac.2022.05.171](https://doi.org/10.1016/j.ijbiomac.2022.05.171).

62 A. R. Ganesan, U. Tiwari, P. Ezhilarasi and G. Rajauria, Application of cold plasma on food matrices: A review on current and future prospects, *J. Food Process. Preserv.*, 2021, **45**, e15070, DOI: [10.1111/jfpp.15070](https://doi.org/10.1111/jfpp.15070).

63 T. Hymavathi, T. P. Roberts, E. Jyothisna and V. T. Sri, Proximate and mineral content of ready to use minor millets, *Int. J. Chem. Stud.*, 2020, **8**, 2120–2123, DOI: [10.22271/chemi.2020.v8.i2af.9065](https://doi.org/10.22271/chemi.2020.v8.i2af.9065).

64 H. Zhang, Z.-Y. Wang, X. Yang, *et al.*, Determination of free amino acids and 18 elements in freeze-dried strawberry and blueberry fruit using an Amino Acid Analyzer and ICP-MS with micro-wave digestion, *Food Chem.*, 2014, **147**, 189–194, DOI: [10.1016/j.foodchem.2013.09.118](https://doi.org/10.1016/j.foodchem.2013.09.118).

65 A. Sarkar, T. Niranjan, G. Patel, A. Kheto, B. K. Tiwari and M. Dwivedi, Impact of cold plasma treatment on nutritional, antinutritional, functional, thermal, rheological, and structural properties of pearl millet flour, *J. Food Process Eng.*, 2023, **46**, e14317, DOI: [10.1111/jfpe.14317](https://doi.org/10.1111/jfpe.14317).

66 J. O. Owheruo, B. O. Ifesan and A. O. Kolawole, Physicochemical properties of malted finger millet (*Eleusine coracana*) and pearl millet (*Pennisetum glaucum*), *Food Sci. Nutr.*, 2019, **7**, 476–482, DOI: [10.1002/fsn3.816](https://doi.org/10.1002/fsn3.816).

